Effects of High Glucose and Advanced Glycation End Products on the Expressions of Sclerostin and RANKL As Well As Apoptosis in Osteocyte-Like MLO-Y4-A2 Cells

Ken-ichiro Tanaka, Toru Yamaguchi, Ippei Kanazawa, Toshitsugu Sugimoto.

Internal Medicine 1, Shimane University Faculty of Medicine, Izufmo 693-8501, Japan.

Email addresses: K Tanaka: ken1nai@med.shimane-u.ac.jp; T Yamaguchi: yamaguch@med.shimane-u.ac.jp; I Kanazawa: ippei.k@med.shimane-u.ac.jp; T Sugimoto: sugimoto@med.shimane-u.ac.jp

To whom correspondence should be addressed: K. Tanaka, MD, Ph.D.

Department of Internal Medicine 1, Shimane University Faculty of Medicine, Izumo, Japan

Phone: +81-853-20-2183, Fax: +81-853-23-8650

E-mail: ken1nai@med.shimane-u.ac.jp

Key words: Advanced glycation end products, Osteocyte, Sclerostin, Receptor activator of nuclear factor-κB ligand, Parathyroid hormone

ABSTRACT

In diabetes mellitus (DM), high glucose (HG) and advanced glycation end products (AGEs) are involved in bone quality deterioration. Osteocytes produce sclerostin and receptor activator of nuclear factor-κB ligand (RANKL) and regulate osteoblast and osteoclast function. However, whether HG or AGEs directly affect osteocytes and regulate sclerostin and RANKL production is unknown. Here, we examined the effects of HG, AGE2, and AGE3 on the expression of sclerostin and RANKL and on apoptosis in osteocyte-like MLO-Y4-A2 cells. Treatment of the cells with 22 mM glucose, 100 μg/mL either AGE2 or AGE3 significantly increased the expression of sclerostin protein and mRNA; however, both AGEs, but not glucose, significantly decreased the expression of RANKL protein and mRNA. Moreover, treatment of the cells with HG, AGE2, or AGE3 for 72 hours induced significant apoptosis. These detrimental effects of HG, AGE2, and AGE3 on sclerostin and RANKL expressions and on apoptosis were antagonized by pretreatment of the cells with 10^{-8} M human parathyroid hormone (PTH)-(1–34). Thus, HG and AGEs likely suppress bone formation by increasing sclerostin expression in osteocytes, whereas AGEs suppress bone resorption by decreasing RANKL expression. Together, these processes may cause low bone turnover in DM. In addition, HG and AGEs may cause cortical bone deterioration by inducing osteocyte apoptosis. PTH may effectively treat these pathological processes and improve osteocyte function.

1. Introduction

Elderly people often have both osteoporosis and diabetes mellitus (DM); notably, the risks of hip and spine fracture are increased in patients with type 1 (T1) or type 2 (T2) DM. In our previous study, the presence of T2DM was a risk factor for prevalent vertebral fractures, with odds ratios of 1.86 in women and 4.73 in men; furthermore, BMD was not useful for assessing vertebral fracture risk in patients with T2DM (1). Thus, BMD does not reflect bone fragility, which is likely involved in the increased fracture risk of patients with T2DM; impaired bone quality likely exists in these populations.

Non-enzymatic reactions of carbohydrates with proteins produce advanced glycation end products (AGEs); the accumulation of AGEs is a characteristic feature of the tissues of elderly people and patients with DM (2). Some complications of DM such as neuropathy, retinopathy, and nephropathy are related to the diverse biological activities of AGEs, especially AGE2 and AGE3 (3-5). AGEs are also known to affect bone tissue. In our previous studies, the combination of high glucose (HG) and AGE2 inhibited the mineralization of osteoblastic MC3T3-E1 cells through a glucose-induced increase in the expression of the AGE receptor (RAGE) (6); moreover, AGE2 and AGE3 inhibited the osteoblastic differentiation or mineralization of mouse stromal ST2 cells by decreasing osterix expression, increasing TGF-β expression, and suppressing endoplasmic reticulum stress proteins (7–9).

In the process of bone remodeling, bone is constantly renewed by the balanced action of osteoblastic bone formation and osteoclastic bone resorption. A receptor activator of nuclear factor-κB ligand (RANKL) is a member of the tumor necrosis factor (TNF) cytokine family which is a ligand for osteoprotegerin and functions as a key factor for osteoclast differentiation and activation (10). Osteocytes account for 90%–95% of bone cells; they are a major source of the osteoclastgenic cytokine RANKL and have a greater capacity to support osteoclastgenesis than do osteoblasts and bone marrow stromal cells (11). In contrast, sclerostin is specifically expressed in osteocytes and inhibits osteoblast function and bone formation by antagonizing canonical Wnt signaling (12). Thus, osteocytes are likely the ‘commander cells’ of bone remodeling by regulating osteoblastgenesis and osteoclastgenesis through RANKL and sclerostin; however, it remains unclear whether HG or AGEs affect osteocytes or regulate the production of these factors, thereby causing

bone deterioration in patients with DM.

In this study, we examine the effects of HG, AGE2, and AGE3 on the expressions of RANKL and sclerostin and on apoptosis in osteocytic MLO-Y4-A2 cells. In addition, we clarify the role of osteocytes in the impaired bone quality of patients with DM.

2. Materials and Methods

2.1. Materials

Human parathyroid hormone (PTH)-(1–34) and an anti-β-actin antibody were obtained from Sigma-Aldrich (St. Louis, MO, USA). Anti-sclerostin antibody was from Abcam (Tokyo, Japan). Anti-RANKL antibody was from Santa Cruz Biotechnology (Santa Cruz, CA, USA). Anti-RAGE antibody was from R&D Systems (Minneapolis, MN, USA). All other chemicals used were of analytical grade.

2.2. Cell culture

Mouse osteocyte-like MLO-Y4-A2 cells in this study were kindly provided by Dr. Y. Kato (AsahiKasei Medical Corporation, Tokyo, Japan), who worked with Prof. Bonewald (University of Missouri) and subcloned the more uniform MLO-Y4-A2 cells from MLO-Y4 cells. Cells were cultured on type I collagen-coated plates in α-MEM containing 5.5 mmol/L glucose. The medium was supplemented with 10% fetal bovine serum (FBS) and 1% penicillin–streptomycin (Gibco-BRL) in 5% CO_2 at 37°C and was changed twice a week.

2.3. Preparation of AGEs

AGEs were prepared as described previously (6). Briefly, AGE2 and AGE3 were prepared by incubating 50 mg/mL BSA (Sigma) with 0.1 M DL-glyceraldehyde (Nacalai Tesque, Kyoto, Japan) and 0.1 M glycolaldehyde (Sigma), respectively, under sterile conditions in 0.2 M phosphate buffer (pH 7.4) containing 5 mM diethylene-triamine-pentaacetic acid at 37 °C for 7 days. As a negative control, nonglycated BSA was incubated under the same conditions except for the absence of DL-glyceraldehyde or glycolaldehyde. Then low-molecular-weight reactants and aldehydes were removed by using PD-10 column chromatography and dialysis against PBS.

2.4. Protein extraction and Western blot analysis

Cells were lysed with radioimmunoprecipitation buffer containing 0.5 mM phenylmethylsulfonylfluoride, complete protease inhibitor mixture (Roche Applied Science, Tokyo, Japan), 1% Triton X-100, and 1 mM sodium orthovanadate. Proteins were transferred in 25 mM Tris, 192 mM glycine, and 20% methanol to polyvinylidene difluoride membrane. Blots were blocked with 20 mM Tris-HCl (pH 7.5), 137 mM NaCl, 0.1% Tween-20, and 3% dried milk powder. The membranes were immunoblotted with each primary antibody. The antigen–antibody complexes were visualized by using the appropriate secondary antibodies (Sigma) and an enhanced chemiluminescence detection system (LAS-4000 IR multi-color imager, FUJIFILM, Tokyo, Japan). The results depicted in each figure are representative of at least three independent cell preparations. Each experiment was repeated three times.

2.5. Quantification of sclerostin and RANKL

The concentrations of sclerostin and RANKL in whole-cell lysates or culture medium was determined by using commercially available diagnostic ELISA kits (R&D Systems, Minneapolis, MN and Abcam Corp., Tokyo, Japan, respectively).

2.6. RNA extraction and real-time PCR

Total RNA was prepared from the cells by using Trizol reagent (Invitrogen, San Diego, CA, USA). cDNA was synthesized by using a SuperScript-III cDNA synthesis kit (Invitrogen). Specific mRNA was quantified by using an ABI PRISM 7000 sequence detection system (Applied Biosystems Inc.) with SYBR Premix Ex TaqTM Π (Perfect Real Time) kits (TaKaRa), according to the manufacturer's standard protocol. The mRNA value for each gene was normalized relative to the mouse GAPDH mRNA levels in RNA samples. Primer sequences (forward and reverse) were as follows: GAPDH, 5′-GTGTACATGGTTCCAGTATGAGTCC-3′ and 5′-AGTGAGTTGTCATATTTCTCGTGGT-3′; SOST, 5′-TCCTCCTGAGAACAACCAGAC-3′ and 5′-TGTCAGGAAGCGGGTGTAGTG-3′; and RANKL, 5′-GGATCACAGCACATCAGAGCAGAG-3′ and 5′-GTAAGGAGGGGTTGGAGACCTCG-3′.

2.7. RT-PCR

For investigating the expression of RAGE mRNA in MLO-Y4-A2 cells and mouse stromal ST2 cells, RT-PCR was performed from the cDNA. Primer sequences for RAGE (forward and reverse) were as follows: 5´-ACAACCAACTCGGACTTCCA-3´ and 5´-GTCGTTTTCGCCACAGGATA-3´. The PCR conditions were 95°C for 15 s, 60°C for 30 s, and 72°C for 1 min for 34 cycles. PCR products were separated by electrophoresis on 2% agarose gels and visualized by ethidium bromide staining with ultraviolet light by using an electronic ultraviolet transilluminator (Toyobo CO. Ltd, Tokyo, Japan).

2.8. siRNA transfection

Mouse RAGE siRNA and control siRNA duplexes were designed and synthesized by Ambion (Austin, TX, USA). MLO-Y4-A2 cells were seeded in 6-well plates and cultured at 37 °C for 48 hours in α-MEM containing 10% FBS and antibiotics, followed by a 24-hour incubation in medium without antibiotics. Cells were transfected with siRNA (50 nM) by using Lipofectamine (Invitrogen), according to the manufacturer's instructions. After another 48 hours of culture, cells were transferred to another plate containing fresh α-MEM supplemented with 10% FBS and antibiotics.

2.9. Measurement of apoptotic cell death

MLO-Y4-A2 cells were seeded on 96-well plates at a density of 3000 cells/well and were incubated overnight in α-MEM with 10% FBS and antibiotics. On the next day, the cells were treated with either BSA (control), HG, AGE2, or AGE3 for 24, 48, and 72 hours. Then the cells were lysed, and the supernatant was analyzed in an ELISA for DNA fragments (Cell Death Detection ELISA Plus, Roche Molecular Biochemicals, Indianapolis, IN, USA).

2.10. Statistics

All experiments were repeated at least three times. Data are expressed as mean ± S.E. Statistical analysis was performed by using analysis of variance. A *P* value of less than 0.05 was taken to indicate a

significant difference.

3. Results

3.1. Effects of HG, AGE2, and AGE3 on the expressions of sclerostin or RANKL in MLO-Y4-A2 cells

We examined the effects of HG, AGE2, and AGE3 on the expression of sclerostin in MLO-Y4-A2 cells. Treatments of the cells with 22 mM HG and 100 μg/mL either AGE2 or AGE3 significantly increased the level of sclerostin protein in whole cell lysates by Western blot analyses (Fig. 1A) and in both whole cell lysates and supernatants by ELISA (Fig. 1B). Treatments of the cells with the HG, AGE2, or AGE3 alone significantly increased the level of sclerostin mRNA by real-time PCR; the combination of HG plus AGE2 or HG plus AGE3 did not show any additive or synergistic affects (Fig. 1C). Next, we examined the effects of HG, AGE2, and AGE3 on the expression of RANKL in MLO-Y4-A2 cells. Treatments of the cells with 100 μg/mL AGE2 or AGE3, but not 22 mM HG, significantly suppressed the level of RANKL protein in whole cell lysates by Western blot analyses (Fig. 1D) and in both whole-cell lysates and supernatants by ELISA (Fig. 1E). Treatment of the cells with either AGE2 or AGE3 alone significantly suppressed the level of RANKL mRNA; however, HG alone or the combination of HG plus AGE2 or HG plus AGE3 did not show any effects (Fig. 1F).

3.2. Expression of RAGE in MLO-Y4-A2 cells and effects of its reduced expression on AGE2- or AGE3-modulated expressions of sclerostin or RANKL

Using mouse stromal ST2 cells as a positive control, we examined the expression of RAGE in MLO-Y4-A2 cells. By using RT-PCR with sequence analysis and Western blotting, we confirmed that RAGE mRNA and protein both were expressed in MLO-Y4-A2 cells (Fig. 2A and B, respectively). Next, we examined the effects of a reduction in RAGE expression by siRNA transfection on AGE2- or AGE3-modulated expressions of sclerostin or RANKL. By western blot analysis, RAGE protein was expressed less in the cells transfected with its siRNA (Fig. 2C). This reduction in RAGE expression suppressed AGE2- or AGE3-induced increases in sclerostin protein in the cells (Fig. 2D); furthermore, it recovered AGE2- or AGE3-induced decreases in RANKL protein (Fig. 2E).

3.3. Effects of human PTH-*(1–34) on HG-, AGE2-, or AGE3-modulated expression of sclerostin or RANKL in MLO-Y4-A2 cells*

Using Western blotting, we examined the effects of human PTH-(1–34) on the HG-, AGE2-, and AGE3-modulated expression of sclerostin or RANKL in MLO-Y4-A2 cells. Pretreatment of the cells with 10^{-8} M human PTH-(1–34) suppressed the basal expression of sclerostin protein and the HG-, AGE2-, or AGE3-induced increases in sclerostin protein (Fig. 3A and B). Furthermore, the inhibitory effects on AGE2- and AGE3-induced ones were dose-dependent at the concentrations of 10^{-10} to 10^{-8} M (Fig. 3C). In contrast, pretreatments of the cells with 10^{-8} M human PTH-(1–34) increased the basal expression of RANKL protein and the AGE2- or AGE3-induced decreases in RANKL protein (Fig. 3D). These effects were also dose-dependent (10^{-10} M–10^{-8} M) (Fig. 3E).

3.4. Effects of HG, AGE2, or AGE3 on the apoptosis of MLO-Y4-A2 cells

We examined the effects of HG, AGE2, or AGE3 on the apoptosis of MLO-Y4-A2 cells. Treatment of the cells with 22 mM HG or 100 μg/mL either AGE2 or AGE3 for 72 hours, but not 24 or 48 hours, significantly induced apoptosis (Fig. 4A). Next, we examined the effects of human PTH-(1–34) on HG-, AGE2-, or AGE3-induced apoptosis. Pretreatment of the cells with 10^{-8} M human PTH-(1–34) significantly reversed AGE2- or AGE3-induced apoptosis (Fig. 4B).

We measured the concentration of RANKL protein in whole-cell lysates and supernatants at 72 hours (when significant apoptosis occurred). Treatment of the cells with 100 μg/mL either AGE2 or AGE3 for 72 hours significantly suppressed the concentration of RANKL protein in whole-cell lysates (Fig. 4C). Although AGE2 or AGE3 treatment significantly increased the concentration of RANKL protein in the supernatant, the absolute value was small; thus, the overall RANKL concentration of the whole-cell lysate plus supernatant was still decreased by AGE2 and AGE3.

4. Discussion

In this study, treatment of osteocyte-like MLO-Y4-A2 cells with HG, AGE2, or AGE3 increased sclerostin expression and suppressed RANKL expression (Fig. 1). In addition, RAGE was expressed in MLO-Y4-A2 cells; a reduction in its expression suppressed the AGE2- or AGE3-induced increase in sclerostin expression and recovered the AGEs-induced decreases in RANKL expression (Fig. 2). Therefore, partly by binding to RAGE in osteocytes, AGE2 and AGE3 suppress bone formation by increasing sclerostin expression and suppress bone resorption by decreasing RANKL expression. According to several studies, serum sclerostin levels are significantly increased in patients with T2DM (13, 14). In an *in vtiro* study in MLO-Y4 cells, 30 mM HG increased sclerostin compared with control levels (15). Furthermore, compared with women without DM, women with DM had significantly decreased bone-resorption markers (16). These experimental and clinical observations about sclerostin increase and low bone resorption in DM are in accord with our present findings.

In this study, treatments of MLO-Y4-A2 cells with HG, AGE2, or AGE3 for 72 hours induced significant apoptosis, which may cause bone fragility (Fig. 4). In T2DM, an increase in cortical porosity plays important roles in bone fragility. Specifically, cortical porosity is increased in postmenopausal patients with T2DM (17). However, the mechanism of increased cortical porosity in T2DM remains unclear. Continuous injection of human PTH-(1–34) increased cortical porosity in 6-month-old female Sprague-Dawley rats (18), suggesting the stimulatory action of PTH in the formation of cortical porosity. However, because high levels of glucose inhibit PTH secretion and patients with DM have lower PTH levels than do their non-DM counterparts (19), factors other than PTH (such as apoptosis of osteocytes and increased RANKL expression) may contribute to the formation of cortical porosity in T2DM. For example, compared with non-alcohol-fed rats, alcohol-fed rats have more intracortical femoral porosities and apoptosis of osteocytes (20). Furthermore, in murine parietal bones, apoptotic bodies derived from MLO-Y4 cells and primary murine osteocytes enhance osteoclastic bone resorption through TNF-α (21). In contrast, mice have significantly increased intracortical femoral porosity when their osteoblasts and osteocytes lack genes essential for apoptosis, such as Bak and Bax (22). Therefore, it is controversial whether apoptosis of osteocytes is involved in the increase in

cortical porosity.

We also evaluated RANKL in our investigation of bone fragility; treatment of MLO-Y4-A2 cells with HG, AGE2, or AGE3 for 72 hours induced a decrease in the total sum of RANKL protein in cell lysates and supernatants. However, according to several studies, increased RANKL expression may cause an increase of cortical porosity. Specifically, overexpression of human RANKL in transgenic mice causes severe cortical bone porosity (23). Furthermore, an anti-RANKL antibody, Denosumab, markedly inhibits cortical porosity in ovariectomized cynomolgus monkeys (24). Although our present RANKL data do not suggest the involvement of osteocytes in the increase in cortical porosity in DM, hyperglycemia and AGEs likely induce the apoptosis of osteocytes (Fig. 4); therefore, these agents may cause cortical bone deterioration in patients with DM.

In our study, PTH had beneficial effects on the expression of sclerostin and RANKL and on the apoptosis of MLO-Y4-A2 cells induced by HG, AGE2, and AGE3 (Fig. 3 and 4). Specifically, PTH suppressed HG-, AGE2-, or AGE3-induced increases in sclerostin expression and recovered AGE2- or AGE3-induced decreases in RANKL expression. PTH also reversed HG-, AGE2-, and AGE3-induced apoptosis of the cells. Similarly, in mice, chronic elevation of PTH reduces sclerostin expression by osteocytes (25). Furthermore, the expression of RANKL in tibial diaphysis is lower in mice lacking the PTH/PTH-related peptide receptor (26). Compared with mice receiving placebo treatment, mice receiving prednisolone have 148% greater apoptosis of their osteocytes; PTH treatment prevents this increase (27). Our findings seem to be in accord with these previous observations of the actions of PTH on bone; therefore, in patients with T2DM, PTH may be effective for treating low bone turnover and cortical bone deterioration by revitalizing bone metabolism and preventing osteocyte apoptosis.

However, this study has some limitations. First, our clonal MLO-Y4-A2 cells may not be identical to natural osteocytes *in vivo*; we need further experiments with cultured primary osteocytes or animals to strengthen the present findings. Second, we did not investigate the signals that mediate the effects of HG, AGE2, or AGE3 on the expressions of sclerostin or RANKL and on apoptosis.

In conclusion, HG, AGE2, and AGE3 suppress bone formation via increased sclerostin expression,

and the AGEs suppress bone resorption via decreased RANKL expression by partly binding to RAGE in osteocyte-like cells. In these cells, HG, AGE2, and AGE3 also induce apoptosis. Notably, these detrimental effects were reversed by pretreatment of the cells with PTH. Therefore, impaired osteocyte function is involved in low bone turnover and cortical bone deterioration in DM; PTH may effectively treat these pathological conditions.

Acknowledgements

This work was supported in part by Grant-in-Aid no. 25460898 (to TY) from the Ministry of Science, Education, and Culture of Japan. Authors' roles: KT and TY conceived and designed the experiments; KT performed the experiments and analyzed the data; IK and TS contributed equipment/materials; KT and TY wrote the paper; and all authors approved the final version.

References

1. Yamamoto M, Yamaguchi T, Yamauchi M, Kaji H, Sugimoto T. Diabetic patients have an increased risk of vertebral fractures independent of BMD or diabetic complications. J Bone Miner Res. 2009; 24(4):702-709.
2. Singh R, Barden A, Mori T, Beilin L. Advanced glycation end-products: a review. Diabetologia. 2001; 44(2):129-146.
3. Sekido H, Suzuki T, Jomori T, Takeuchi M, Yabe-Nishimura C, Yagihashi S. Reduced cell replication and induction of apoptosis by advanced glycation end products in rat Schwann cells. Biochem Biophys Res Commun. 2004; 320(1):241-248.
4. Yamagishi S, Amano S, Inagaki Y, Okamoto T, Takeuchi M, Makita Z. Beraprost sodium, a prostaglandin I2 analogue, protects against advanced glycation end products-induced injury in cultured retinal pericytes. Mol Med. 2002; 8(9):546-550.
5. Yamagishi S, Inagaki Y, Okamoto T, Amano S, Koga K, Takeuchi M, Makita Z. Advanced glycation end product-induced apoptosis and overexpression of vascular endothelial growth factor and monocyte chemoattractant protein-1 in human-cultured mesangial cells. J Biol Chem. 2002; 277(23):20309-20315.
6. Ogawa N, Yamaguchi T, Yano S, Yamauchi M, Yamamoto M, Sugimoto T. The combination of high glucose and advanced glycation end-products (AGEs) inhibits the mineralization of osteoblastic MC3T3-E1 cells through glucose-induced increase in the receptor for AGEs. Horm Metab Res. 2007; 39(12):871-875.
7. Okazaki K, Yamaguchi T, Tanaka K, Notsu M, Ogawa N, Yano S, Sugimoto T. Advanced glycation end products (AGEs), but not high glucose, inhibit the osteoblastic differentiation of mouse stromal ST2 cells through the suppression of osterix expression, and inhibit cell growth and increasing cell apoptosis. Calcif Tissue Int. 2012; 91(4):286-296.
8. Tanaka K, Yamaguchi T, Kaji H, Kanazawa I, Sugimoto T. Advanced glycation end products suppress osteoblastic differentiation of stromal cells by activating endoplasmic reticulum stress. Biochem Biophys Res Commun. 2013; 438(3):463-467.

9. Notsu M, Yamaguchi T, Okazaki K, Tanaka KI, Ogawa N, Kanazawa I, Sugimoto T. Advanced Glycation End Product 3 (AGE3) Suppresses the Mineralization of Mouse Stromal ST2 Cells and Human Mesenchymal Stem Cells by Increasing TGF-β Expression and Secretion. Endocrinology. 2014 [Epub ahead of print]
10. Yasuda H, Shima N, Nakagawa N, Yamaguchi K, Kinosaki M, Mochizuki S, Tomoyasu A, Yano K, Goto M, Murakami A, Tsuda E, Morinaga T, Higashio K, Udagawa N, Takahashi N, Suda T. Osteoclast differentiation factor is a ligand for osteoprotegerin/osteoclastogenesis-inhibitory factor and is identical to TRANCE/RANKL. Proc Natl Acad Sci U S A. 1998; 95(7):3597-3602.
11. Nakashima T, Hayashi M, Fukunaga T, Kurata K, Oh-Hora M, Feng JQ, Bonewald LF, Kodama T, Wutz A, Wagner EF, Penninger JM, Takayanagi H. Evidence for osteocyte regulation of bone homeostasis through RANKL expression. Nat Med. 2011; 17(10):1231-1234.
12. Winkler DG, Sutherland MK, Geoghegan JC, Yu C, Hayes T, Skonier JE, Shpektor D, Jonas M, Kovacevich BR, Staehling-Hampton K, Appleby M, Brunkow ME, Latham JA. Osteocyte control of bone formation via sclerostin, a novel BMP antagonist. EMBO J. 2003; 22(23):6267-6276.
13. García-Martín A, Rozas-Moreno P, Reyes-García R, Morales-Santana S, García-Fontana B, García-Salcedo JA, Muñoz-Torres M. Circulating levels of sclerostin are increased in patients with type 2 diabetes mellitus. J Clin Endocrinol Metab. 2012; 97(1):234-241.
14. Yamamoto M, Yamauchi M, Sugimoto T. Elevated sclerostin levels are associated with vertebral fractures in patients with type 2 diabetes mellitus. J Clin Endocrinol Metab. 2013; 98(10):4030-4037.
15. Kim JY, Lee SK, Jo KJ, Song DY, Lim DM, Park KY, Bonewald LF, Kim BJ. Exendin-4 increases bone mineral density in type 2 diabetic OLETF rats potentially through the down-regulation of SOST/sclerostin in osteocytes. Life Sci. 2013; 92(10):533-540.
16. Gerdhem P, Isaksson A, Akesson K, Obrant KJ. Increased bone density and decreased bone turnover, but no evident alteration of fracture susceptibility in elderly women with diabetes mellitus. Osteoporos Int. 2005; 16(12):1506-1512.
17. Patsch JM, Burghardt AJ, Yap SP, Baum T, Schwartz AV, Joseph GB, Link TM. Increased cortical

porosity in type 2 diabetic postmenopausal women with fragility fractures. J Bone Miner Res. 2013 ;28(2):313-324.

18. Lotinun S, Evans GL, Bronk JT, Bolander ME, Wronski TJ, Ritman EL, Turner RT. Continuous parathyroid hormone induces cortical porosity in the rat: effects on bone turnover and mechanical properties. J Bone Miner Res. 2004; 19(7):1165-1171.
19. Sugimoto T, Ritter C, Morrissey J, Hayes C, Slatopolsky E. Effects of high concentrations of glucose on PTH secretion in parathyroid cells. Kidney Int. 1990; 37(6):1522-1527.
20. Maurel DB, Boisseau N, Pallu S, Rochefort GY, Benhamou CL, Jaffre C. Regular exercise limits alcohol effects on trabecular, cortical thickness and porosity, and osteocyte apoptosis in the rat. Joint Bone Spine. 2013; 80(5):492-498.
21. Kogianni G, Mann V, Noble BS. Apoptotic bodies convey activity capable of initiating osteoclastogenesis and localized bone destruction. J Bone Miner Res. 2008; 23(6):915-927.
22. Jilka RL, O'Brien CA, Roberson PK, Bonewald LF, Weinstein RS, Manolagas SC. Dysapoptosis of osteoblasts and osteocytes increases cancellous bone formation but exaggerates cortical porosity with age. J Bone Miner Res. 2014; 29(1):103-117.
23. Kostenuik PJ, Smith SY, Jolette J, Schroeder J, Pyrah I, Ominsky MS. Decreased bone remodeling and porosity are associated with improved bone strength in ovariectomized cynomolgus monkeys treated with denosumab, a fully human RANKL antibody. Bone. 2011; 49(2):151-161.
24. Kostenuik PJ, Smith SY, Jolette J, Schroeder J, Pyrah I, Ominsky MS. Decreased bone remodeling and porosity are associated with improved bone strength in ovariectomized cynomolgus monkeys treated with denosumab, a fully human RANKL antibody. Bone. 2011; 49(2):151-161.
25. Bellido T, Ali AA, Gubrij I, Plotkin LI, Fu Q, O'Brien CA, Manolagas SC, Jilka RL. Chronic elevation of parathyroid hormone in mice reduces expression of sclerostin by osteocytes: a novel mechanism for hormonal control of osteoblastogenesis. Endocrinology. 2005; 146(11):4577-4583.
26. Tu X, Edwards R, Olivos N, Benson JD, Galli C, Pellegrini G. Conditional deletion of the parathyroid hormone (PTH) receptor 1 from osteocytes results in decreased bone resorption and a progressive

increase in cancellous bone mass. J Bone Miner Res. 2011; 25:S16.

27. Weinstein RS, Jilka RL, Almeida M, Roberson PK, Manolagas SC. Intermittent parathyroid hormone administration counteracts the adverse effects of glucocorticoids on osteoblast and osteocyte viability, bone formation, and strength in mice. Endocrinology. 2010; 151(6):2641-2649.

Figure Legends

Fig. 1. Effects of HG, AGE2, and AGE3 on the expression of sclerostin or RANKL in MLO-Y4-A2 cells.

All reagents were added after the cells reached confluence. (A and D) Control BSA, AGE2, AGE3, and HG were added for 48 hours. Western blot analyses for β-actin, sclerostin, or RANKL were performed on total protein extracts. (B and E) Control BSA, AGE2, AGE3 and HG were added for 48 hours. Sclerostin or RANKL proteins were quantified from whole cell lysates by ELISA. Results are expressed as the mean ± SEM (n = 6). $^{**}P < 0.01$ compared with control. (C and F) AGE2, AGE3, and HG were added separately or together for 24 hours. Real-time PCR for sclerostin or RANKL was performed on total RNA. Data are expressed relative to the GAPDH mRNA value. $^{**}P < 0.01$ compared with control.

Fig. 2. Expression of RAGE in MLO-Y4-A2 cells and effects of its reduced expression on AGE2- or AGE3-modulated expression of sclerostin or RANKL.

(A) Expressions of RAGE mRNA in ST2 cells (positive control) and MLO-Y4-A2 cells by RT-PCR. (B) Expressions of RAGE proteins in ST2 cells and MLO-Y4-A2 cells. Western blot analyses for RAGE were performed on total protein extracts. (C) Effects of RAGE siRNA transfection on its protein expression in MLO-Y4-A2 cells. The cells were transfected with RAGE siRNAs (50 nM) by using Lipofectamine. Total protein was extracted on day 3, and Western blot analyses for RAGE and β-actin were performed. (D and E) After reaching confluence, MLO-Y4-A2 cells were transfected by 50 nM either control siRNA or RAGE siRNA, and then 100 μg/mL either AGE2 or AGE3 were added for 48 hours in α-MEM medium. Total protein was extracted and Western blot analyses for sclerostin, RANKL, and β-actin were performed.

Fig. 3. Effects of human PTH-(1–34) on HG-, AGE2-, and AGE3-modulated expressions of sclerostin or RANKL in MLO-Y4-A2 cells.

(A and B) HG, control BSA, AGE2, and AGE3 were added for 48 hours after pretreatments of human PTH-(1–34) for 24 hours. Western blot analyses for sclerostin and β-actin were performed on total protein extracts. (C) AGE2 and AGE3 were added for 48 hours after pretreatment of human PTH-(1–34) for 24 hours.

Western blot analyses for sclerostin and β-actin were performed on total protein extracts. (D) Control BSA, AGE2, and AGE3 were added for 48 hours after pretreatment of human PTH-(1–34) for 24 hours. Western blot analyses for RANKL and β-actin were performed on total protein extracts. (E) AGE2 and AGE3 were added for 48 hours after pretreatment of human PTH-(1–34) for 24 hours. Western blot analyses for RANKL and β-actin were performed on total protein extracts. The results are representative of three separate experiments.

Fig. 4. Effects of HG, AGE2, and AGE3 on the apoptosis of MLO-Y4-A2 cells.

(A) Cells were treated with AGE2, AGE3, or HG for 24, 48, or 72 hours. (B) Cells were treated with AGE2, AGE3, or HG for 72 hours after pretreatments with human PTH-(1–34) for 24 hours. Apoptosis was analyzed by an ELISA for DNA. $^{**}P < 0.01$ compared with control. The results are representative of three separate experiments and are expressed as the mean ± SEM over control values (n = 6). (C) Effects of apoptosis on the concentration of RANKL of whole-cell lysates and supernatants. Control BSA, AGE2, AGE3, or HG were added for 72 hours after the cells reached confluence. RANKL protein was quantified by ELISA on whole-cell lysates or supernatants. Results are expressed as the mean ± SEM (n = 6). $^{**}P < 0.01$ compared with control.

Figure 1

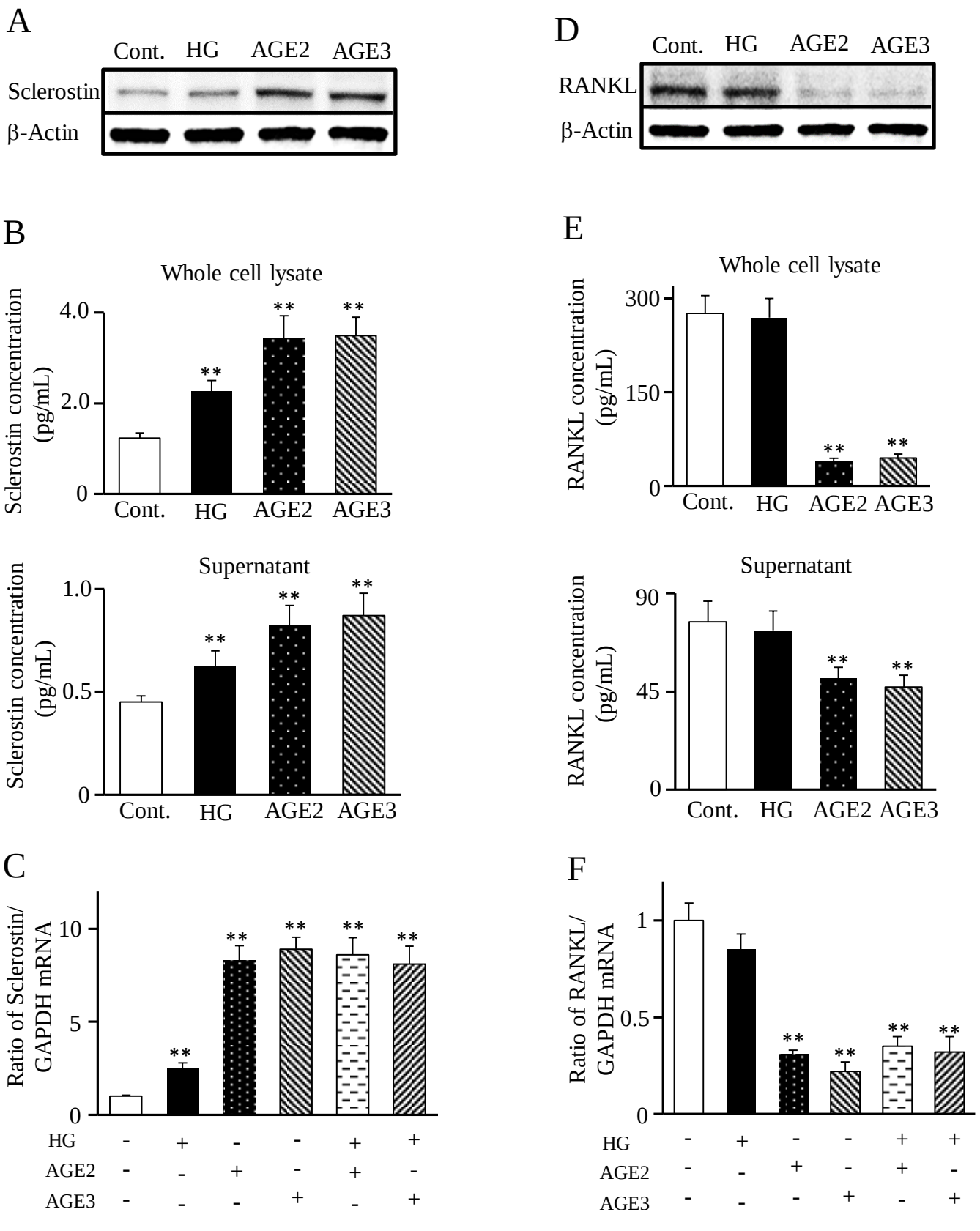
A
Cont.
HG
AGE2
AGE3
Sclerostin
β-Actin
D
Cont.
HG
AGE2
AGE3
RANKL
β-Actin
B
Whole cell lysate
Sclerostin concentration (pg/mL)
4.0
2.0
0
**
Cont.
HG
AGE2
AGE3
Supernatant
Sclerostin concentration (pg/mL)
1.0
0.5
0
**
Cont.
HG
AGE2
AGE3
E
Whole cell lysate
RANKL concentration (pg/mL)
300
150
0
**
Cont.
HG
AGE2
AGE3
Supernatant
RANKL concentration (pg/mL)
90
45
0
**
Cont.
HG
AGE2
AGE3
C
Ratio of Sclerostin/ GAPDH mRNA
10
5
0
**
HG - + - - + +
AGE2 - - + - + -
AGE3 - - - + - +
F
Ratio of RANKL/ GAPDH mRNA
1
0.5
0
**
HG - + - - + +
AGE2 - - + - + -
AGE3 - - - + - +

Figure 2

A

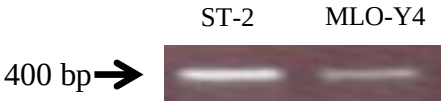

B

C

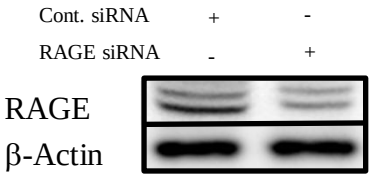

D

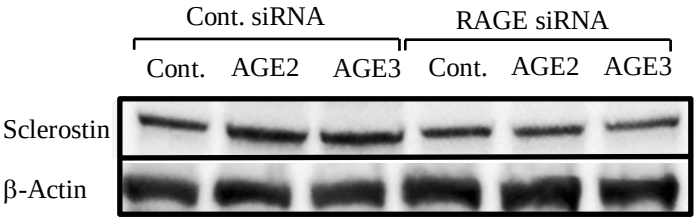

E

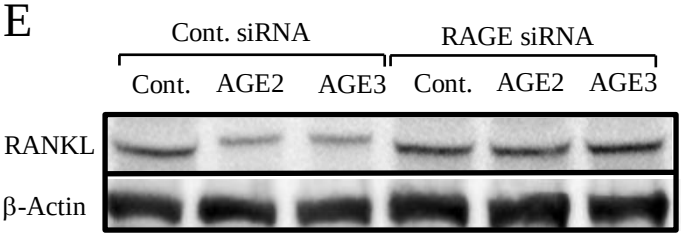

Figure 3

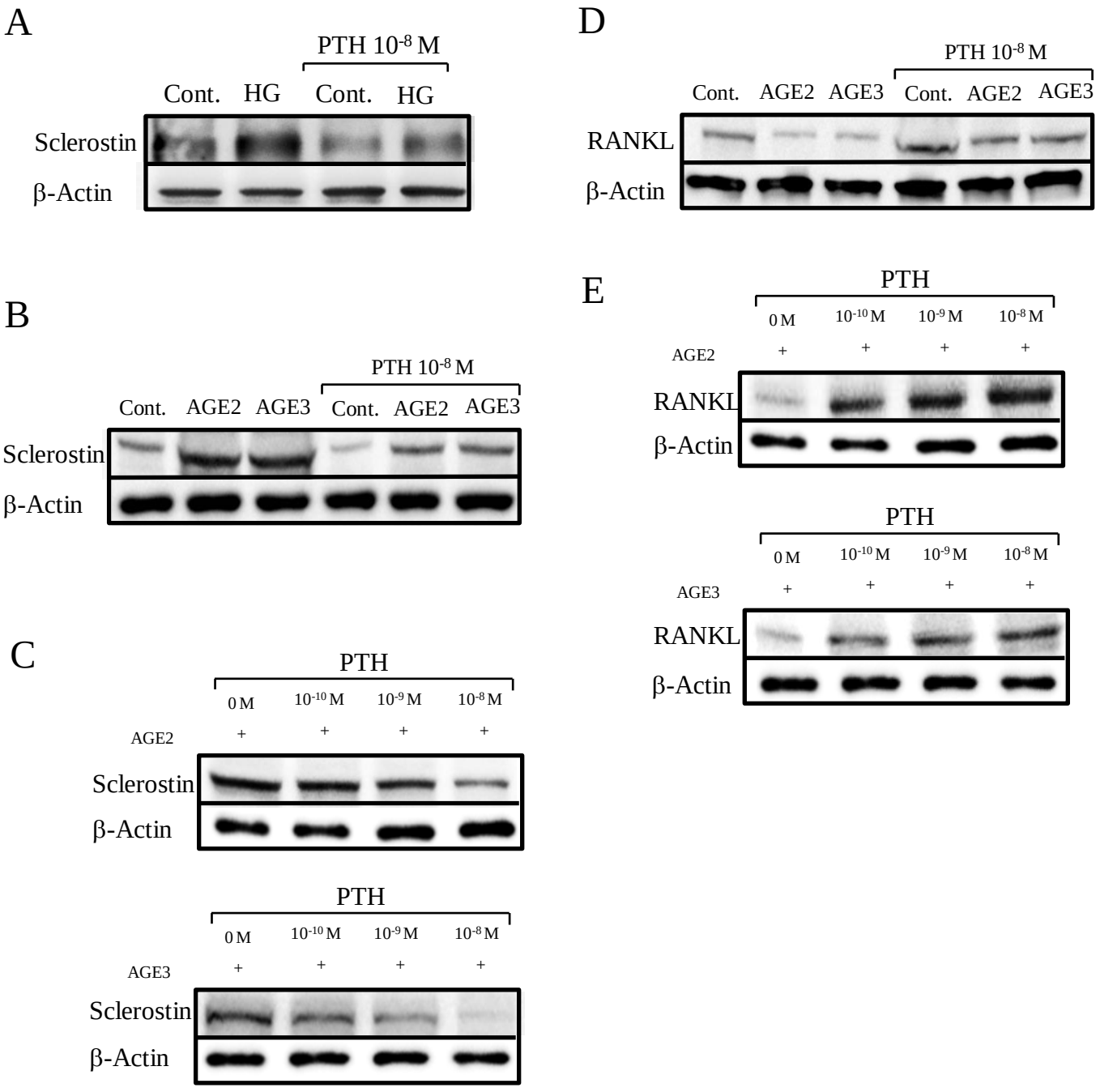
A
PTH 10-8 M
Cont.
HG
Cont.
HG
Sclerostin
β-Actin
B
PTH 10-8 M
Cont.
AGE2
AGE3
Cont.
AGE2
AGE3
Sclerostin
β-Actin
C
PTH
0 M
10-10 M
10-9 M
10-8 M
AGE2
+
Sclerostin
β-Actin
PTH
0 M
10-10 M
10-9 M
10-8 M
AGE3
+
Sclerostin
β-Actin
D
PTH 10-8 M
Cont.
AGE2
AGE3
Cont.
AGE2
AGE3
RANKL
β-Actin
E
PTH
0 M
10-10 M
10-9 M
10-8 M
AGE2
+
RANKL
β-Actin
PTH
0 M
10-10 M
10-9 M
10-8 M
AGE3
+
RANKL
β-Actin

Figure 4

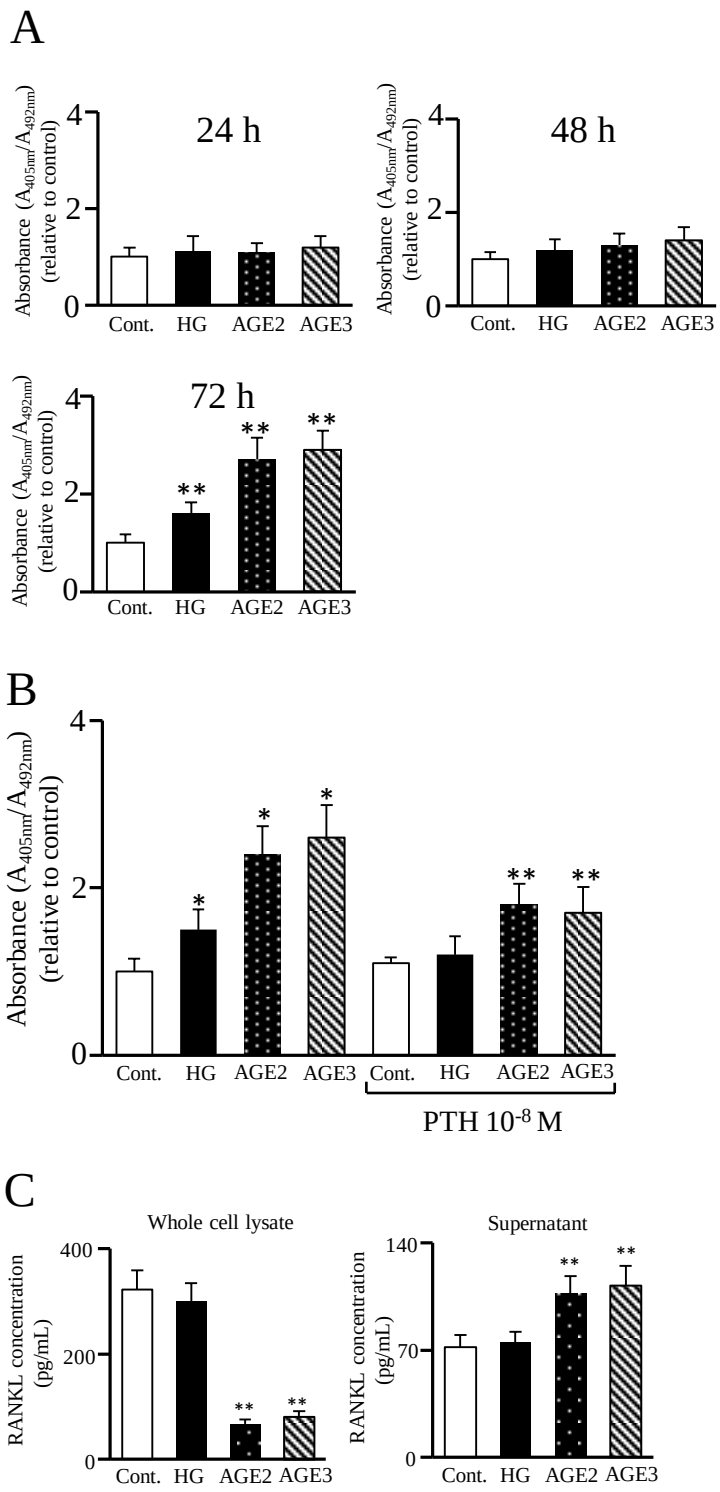
A
24 h
48 h
72 h
Absorbance (A405nm/A492nm) (relative to control)
Cont.
HG
AGE2
AGE3
B
PTH 10-8 M
C
Whole cell lysate
Supernatant
RANKL concentration (pg/mL)